Structural Order and Vibrational Relaxation of Phenylacetylene in Benzene in Liquid Solutions and Frozen Matrices at Low Temperatures. Raman Spectra of Phenylacetylene in Benzene at 77 K

H. Abramczyk,* G. Waliszewska, and B. Brozek

Technical University, Institute of Applied Radiation Chemistry, 93-59 Lódz, Wróblewskiego Street 15, Poland

Received: March 3, 1999

Raman spectra of the ν_S(C≡C) stretching mode of phenylacetylene (PA) dissolved in benzene have been recorded in liquid solutions at room temperature and in solid-state frozen matrixes at 77 K as a function of concentration. The spectra at low temperature reveal spectacular changes in comparison with those observed in liquid solutions. The results given in this paper illustrate the change of the mechanisms of vibrational relaxation due to structural reorganization around the molecular oscillator due to different molecular environments.

1. Introduction

The acetylene (tolane) linkage X−C≡C−Y is often used in liquid crystal materials, including those that exhibit the nematic phase and smectic phases. The acetylene linkage is a conjugative linking group between the core units that enhances the longitudinal polarizability and extends the molecular length while linearity is maintained. The nematic phase stability of tolane is much higher than the parent cyanobiphenyls, well-known nematogenics and the first commercially available liquid crystals for use in display devices.

The phenylacetylene derivatives with many different types of lateral substituents have been used (F, Cl, CN, CH_3). However, the fluoro substituent is the most useful because of its subtle combination of small size and high electronegativity. Some phenylacetylenes are of particular interest with regard to the most recent liquid crystal technology which uses fluorinated diphenylacetylene (DPA) to achieve high-purity nematic materials.[1]

The most commonly accepted hypothesis is that the nematic phase is generated because of the anisotropy of the polarizability resulting from the conjugated core units and that the higher the polarizability anisotropy the higher the nematic phase stability. However, more and more nematic and smectic materials are synthesized where the cores are constructed solely of alicyclic rings. Hence, the relationship between polarizability and liquid crystal phase stability is still unclear.

The Raman technique is very sensitive to changes in intermolecular structure that accompany transitions from the isotropic liquid phase through liquid crystalline phases with increasingly higher positional order to the crystalline solid. These structural changes are reflected in frequency shifts and sometimes drastic changes in intensities and line widths of the vibrational bands, leading to the disappearance of some bands and the appearance of new ones that have been observed.

Raman line shape analysis yields valuable insight into the structure around the molecular oscillator and the dynamics of the vibrational energy state. The Raman line shape study can also yield meaningful information about the orientational order from the comparison between the VV and VH polarized spectra, and the second-order Legandre polynomial $P_2(\cos \Theta)$ can be obtained, which yields a specification of the degree of order in terms of the so-called order parameter S.[2]

We started our studies on liquid crystal materials with phenylacetylene derivatives without any lateral substituents and the terminal chains: diphenylacetylene[3] and phenylacetylene[4,5] at room temperature and at 77 K in methylcyclohexane and acetonitrile solutions.

In this paper we present Raman spectra for phenylacetylene in benzene in frozen matrixes at 77 K as a function of concentration and compare them with the spectra of their liquids counterparts. The results show spectacular changes and illustrate that Raman spectroscopy is very useful for monitoring structural order going from isotropic liquids to solid-state phases at low temperatures.

A great deal of effort has to be expended in order to establish the connections between vibrational spectra on one hand and molecular properties and intermolecular interactions in liquids, liquid crystals, glasses, and crystals on the other. One of the goals of the proposed work is to develop such connections through systematic Raman and IR studies and theoretical modeling. Since several aspects of the Raman and IR spectra of diphenylacetylene in solutions and solid matrixes obtained by Abramczyk and co-workers[3] are not well-understood, we have studied the Raman and IR spectra of phenylacetylene in solutions and solid matrixes.[4,5] The results demonstrate drastic changes occurring in the C≡C stretch Raman bands of PA as a function of temperature. The bands also exhibit strong solvent dependence.

The results on vibrational properties of the acetylene linkage obtained so far, which show particularly striking effects occurring at low temperatures, encouraged us to do further studies. These effects are extremely sensitive to the kind of solvent. In this paper we have continued our studies on vibrational dynamics of phenylacetylene in another solvent, benzene, at low temperatures and at room temperatures as a function of solution concentration.

The goal of the proposed research is to uncover the molecular basis for the observed behavior and to obtain a more complete picture of the structure and vibrational dynamics of PA in

* Corresponding author. E-mail: abramczy@mitr.p.lodz.pl.

10.1021/jp990751r CCC: $18.00
Published on Web 09/03/1999

different condensed-phase environments. Vibrational spectroscopy will also be used to determine if these molecules exhibit liquid crystalline phases and, if they do, to characterize them. As far as we know the Raman spectra of phenylacetylene at low temperatures have been reported for the first time in our previous paper.[5]

2. Experiment

Spectrograde benzene and phenylacetylene were purchased from Aldrich. Benzene was used without further purification. Phenylacetylene was distillated in a vacuum before preparing solutions. The solutions of PA in benzene were made with concentrations varied for the phenylacetylene mole fraction from $x_{PA} = 0.0$ to 1.0. Raman spectra were measured with Ramanor U1000 (Jobin Yvon) and Spectra Physics 2017S argon ion laser operating at 514 nm. The C≡C stretching mode of PA in benzene was measured. Spectra were recorded at room temperature and at 77 K in a liquid nitrogen bath cryostat. The samples at 77 K were prepared in two different ways: through rapid freezing by suddenly immersing the sample in liquid nitrogen and by slow freezing with the temperature going down gradually at the average cooling rate of 0.5 °C/min. The samples were cooled in commercial glass ampules of approximately 1 cm diameter and 1 mL solution volume. The samples at 293 K were transparent, while the samples at 77 K were much more opaque, although a small part of the laser beam penetrated the whole length of the sample. The spectral slit width was 1.3 cm^{-1} both at room temperature and at 77 K, which corresponds to the 200 μm mechanical slit of the spectrometer.

The signal-to-noise ratio in liquid solutions is about 70:1. A similar ratio is observed in frozen matrixes at higher concentration of PA, whereas at lower concentrations the ratio is lower, being about 20:1 in the worst cases. The smaller ratios come from the fact that measurements in the cryostat always give lower intensities of the signals than in the standard liquid couvette and going to 77 K the intensity decreases drastically in comparison with the liquid phase. The sudden decrease of the Raman band intensities occurs at around 200 K for PA in benzene solutions and slightly depends on concentration. As 200 K is far below the freezing point for these solutions, we believe that the observed VV and VH intensity changes are not related to the sample quality (e.g., stress birefringence) but are indicative of thermotropic mesophases and the increasing degree of anisotropy due to structural ordering. A polarization analyzer and $\lambda/4$ waveplate were used to select polarized (VV) and depolarized (VH) components. The isotropic Raman spectra were calculated according to the relation

$$I_{iso} = I_{VV} - \frac{4}{3} I_{VH}$$

The depolarization ratio defined as

$$P = \frac{I_{VH}}{I_{VV}}$$

was measured for each sample.

The interference filter was used to purify the laser line by removing additional natural emission lines which interfere with the Raman lines, especially in the case of solid samples.

The experimental errors are lower than 0.5 cm^{-1} for the measured line shifts and widths and lower than 20% for depolarization ratios. The baseline errors coming from the background are negligible as the vibrational mode under study is very well separated from the other bands and the background intensity is very low both at 293 and 77 K, indicating the negligible role of multiple elastic scattering.

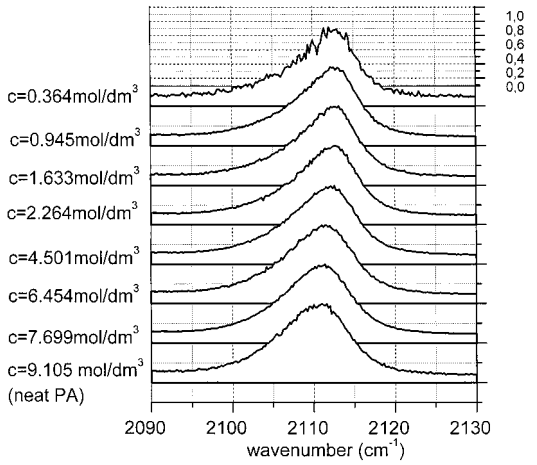

Figure 1. Isotropic Raman spectra of the C≡C stretching mode of phenylacetylene in benzene at room temperature at a few concentrations (c = 0.364, 0.945, 1.633, 2.264, 4.501, 6.454, 7.699, 9.105 mol/dm^3 going from top to bottom).

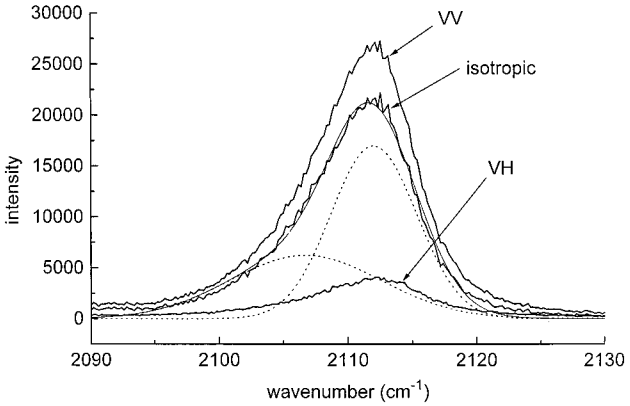

Figure 2. VV, VH, and isotropic Raman spectra of the C≡C stretching mode of phenylacetylene in benzene (c = 4.501 mol/dm^3) at room temperature: - - -, isotropic component after deconvolution into two Gaussians.

3. Results

In this section we present the results of Raman studies on vibrational dynamics of phenylacetylene in benzene as a function of solution concentration at room temperature and at 77 K.

Figure 1 shows the isotropic Raman spectra components of the stretching mode ν_S(C≡C) of phenylacetylene in benzene at room temperature at a few concentrations. In all cases the bands are slightly asymmetric on the low-frequency side. The VV and VH components have similar shapes and change in a similar way with concentration.

In Figure 2 we show the typical VV, VH, and isotropic Raman spectra components of the stretching mode ν_S(C≡C) of phenylacetylene in benzene at room temperature at c = 4.501 mol/dm^3. The best fits were obtained with two Gaussian bands for all the concentrations. The depolarization ratios are the same for both Gaussians within the experimental error.

In Figure 3 the isotropic Raman maximum peak positions ν_0 for both Gaussian bands of the ν_S(C≡C) mode of phenylacetylene in benzene are shown as a function of phenylacetylene mole fraction, x_{PA}. For both bands the maximum peak positions decrease slightly with increasing phenylacetylene concentration,

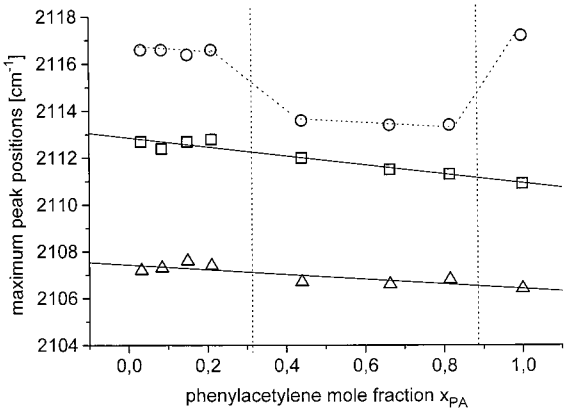

Figure 3. Raman isotropic maximum peak position of the C≡C stretching mode of phenylacetylene in benzene as a function of phenylacetylene mole fraction x_{PA} at room temperature and at 77 K: □, experimental data at room temperature for the higher frequency band (2111 cm^{-1}); —, fitting of experimental data (ν_0(cm^{-1}) = 2112.86 − 1.93x_{PA}); △, experimental data at room temperature for the lower frequency band (2106 cm^{-1}); ···, fitting of experimental data (ν_0(cm^{-1}) = 2107.43 − 1.02x_{PA}); ○, experimental data at 77 K for the higher frequency band.

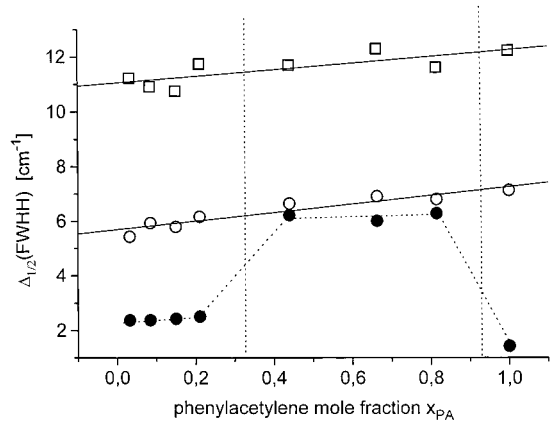

Figure 4. Raman isotropic bandwidth $\Delta_{1/2}$(fwhh) of the C≡C stretching mode of phenylacetylene in benzene as a function of phenylacetylene mole fraction x_{PA} at room temperature and at 77 K: ○, experimental data at room temperature for the higher frequency band (2111 cm^{-1}); —, fitting of experimental data ($\Delta_{1/2}$(fwhh)(cm^{-1}) = 5.69 + 1.54x_{PA}); □, experimental data at room temperature for the lower frequency band (2106 cm^{-1}); ···, fitting of experimental data ($\Delta_{1/2}$(fwhh)(cm^{-1}) = 11.06 + 1.19x_{PA}); ●, experimental data for the higher frequency band at 77 K.

in contrast to the significant decrease in nonpolar methylcyclohexane.[4] The frequency shift in benzene when going from x_{PA} = 0 to 1 is only 1.02 and 1.93 cm^{-1} for both Gaussians, respectively. In comparison, the frequency shift for methylcyclohexane is 6.37 cm^{-1}.[4]

The concentration dependence of the isotropic Raman peak positions were fitted with the linear equations: $\nu_0^{(1)}$(cm^{-1}) = 2107.43 − 1.02x_{PA} and $\nu_0^{(2)}$(cm^{-1}) = 2112.86 − 1.93x_{PA}, respectively.

In Figure 4 the isotropic Raman bandwidths $\Delta_{1/2}$(fwhh)(cm^{-1}) (full width at half-height) of the ν_S(C≡C) mode of phenylacetylene in benzene at room temperature fitted with two Gaussian bands are shown as a function of phenylacetylene mole fraction x_{PA}. For both bands the bandwidths increase slightly with increasing phenylacetylene concentration. The concentration dependence of the isotropic Raman bandwidths was fitted with the linear equations $\Delta_{1/2}^{(1)}$(cm^{-1}) = 11.06 + 1.19x_{PA} and $\Delta_{1/2}^{(2)}$(cm^{-1}) = 5.69 + 1.54x_{PA}.

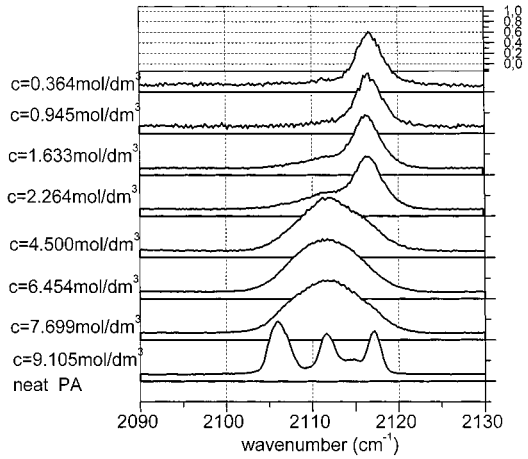

Figure 5. VV Raman spectra of the C≡C stretching mode of phenylacetylene in benzene at 77 K at a few concentrations (rapid freezing) (c = 0.364, 0.945, 1.633, 2.264, 4.501, 6.454, 7.699, 9.105 mol/dm^3 going from top to bottom).

Figure 5 shows the VV Raman spectra of the stretching mode ν_S(C≡C) of phenylacetylene in benzene at 77 K at the same concentrations as shown in Figure 1. The comparison between Figures 1 and 5 shows that the Raman spectra going from the liquid solutions to the frozen matrixes at 77 K change dramatically. The most spectacular change is observed in neat phenylacetylene. The broad asymmetric low-frequency band which is observed in liquid phase at room temperature (Figure 1) becomes split into three narrow bands in the solid-state phase at 77 K (Figure 5).

The second important finding that can be stated from the comparison between Figures 1 and 5 is the significant change of the band shape with dilution at 77 K, contrary to the band shapes in liquid solutions, where all the parameters characterizing the band shape like the maximum peak position, bandwidth, and the profile shape change gradually with dilution (Figures 3 and 4). In contrast, at 77 K we observe the spectacular change of the bandwidth, the maximum peak position, and the band shape with PA concentration. At lower concentrations (c = 0.364−0.945 mol/dm^3) (Figure 5) we observe a single narrow peak with the maximum at about 2116 cm^{-1}, which is blue-shifted by about 4 cm^{-1} with respect to that observed in the liquid phase at the same concentrations. At higher concentrations (c = 1.63−2.264 mol/dm^3) the band still remains narrow at the same maximum position, but the increase of intensity at the low-frequency side can be observed. The intensity increase at the low-frequency side leads to the band broadening and to the red-shift of the maximum peak position (2111 cm^{-1}). In the concentration range between 4.501 and 7.699 mol/dm^3 both the bandwidth and the maximum peak position are similar to those observed in the liquid phase at room temperature. Then, at larger concentrations the broad band begins to split into three peaks. In fact, the deconvolution procedure shown in Figure 6 demonstrates that there are four Gaussian components instead of three.

The changes of the bandwidth and the maximum peak position with PA concentration in benzene at 77 K are shown in Figures 3 and 4. We can see that there are two characteristic concentration regions, at around x_{PA} = 0.3 and 0.9, where the Raman band profile parameters change dramatically.

The third interesting feature which is revealed from the comparison between Figures 2 and 6 is the marked difference in intensities of VV, VH, and isotropic components in the liquid phase and in its solid counterpart. Indeed, the intensity of the

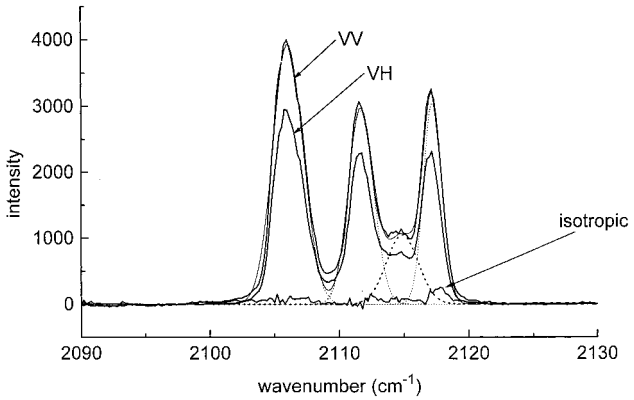

Figure 6. VV, VH, and isotropic Raman spectra of the C≡C stretching mode of neat phenylacetylene at 77 K: - - -, VV component after deconvolution into four Gaussians.

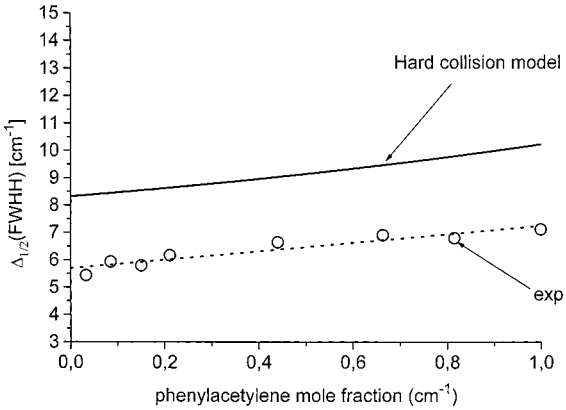

Figure 7. Raman isotropic bandwidth $\Delta_{1/2}$(fwhh) of the C≡C stretching mode of phenylacetylene in benzene as a function of phenylacetylene mole fraction x_{PA}: ○, experimental data at room temperature; —, hard collision theoretical model.[11,12]

isotropic component decreases drastically at 77 K in comparison to that in the liquid phase, as illustrated by the magnitudes of the depolarization ratios. The depolarization ratio increases markedly from 0.147 in liquid benzene to 0.735 in frozen matrix, which means that the isotropic component practically disappears. This feature is observed for all the concentrations.

4. Discussion

The experimental results presented in the paper show that Raman band shape analysis provides an excellent method for monitoring structural order going from isotropic liquids to solid-state phases. It is evident that the changes observed in the Raman band profiles for PA in benzene must illustrate the change of the mechanisms of vibrational relaxation due to structural reorganization or phase transitions.

The study of Raman line shape can provide information on vibrational dynamics, mainly vibrational dephasing (T_2^*), which may occur by a pure dephasing (T_2) and/or by energy relaxation (T_1). In pure dephasing relaxation, dynamic fluctuations of the oscillator frequency destroy the phase relationship. The dephasing caused by T_1 relaxation results from the change of the oscillator phase during the energy exchange, which occurs in the process of depopulation of vibrational states. As both the frequency fluctuations and energy relaxation are due to intra- and intermolecular interactions of the oscillator with the surrounding molecules, the dephasing provides information about the dynamics of interactions and molecular motions around the oscillator. The Raman line shape study can yield meaningful information about the vibrational dynamics only if the vibrational band is homogeneously broadened by dephasing relaxation and not by inhomogeneous broadening. On the other hand, if the line width is dominated by inhomogeneous broadening, we can monitor structural disorder in the liquid phase and inhomogeneities in crystals and glasses at low temperatures.

The vibrational dynamics of liquids is fairly well-understood, and theoretical models and computer simulations dealing with the vibrational states in liquids and their interactions exist in the literature.[4,6−18] In liquids the fast vibrational dephasing accounts for a dominant part of the homogeneous line width at ambient temperature.[18] However, under certain circumstances, vibrational line shapes are dominated by inhomogeneous broadening.[19,20] The theoretical models for liquids use the concept of vibrations localized on molecules treated as the statistical ensemble and involving the ensemble-averaged density matrix of the individual molecules.[14−18]

The theoretical models of vibrational dephasing in crystals use a quantum mechanical rather than a statistical framework in treating the collection of molecules in the sample and apply the Frenkel exciton formalism[21−25] in the interpretation of experimental data. The intramolecular vibrational states are considered to be extended crystal states due to the periodicity of the crystal state Hamiltonian rather than being localized on each molecule. Molecular crystals have traditionally fulfilled the role of model systems for understanding of the dissipation of excess vibrational energy in solid-state phase. In some molecular crystals such as naphthalene[22] the T_2 processes at low temperatures are negligible and the homogeneous line broadening is dominated by T_1 processes.

Much less is known about vibrational relaxation in glasses. Vibrational relaxation in the glass phases at low-temperature frozen matrixes can be vastly different from its liquid and crystal counterparts. Not only the energy relaxation T_1 but also the phase relaxation T_2 can differ due to the effects of interactions of the solute with the solvent molecules and the different time scale of these processes. The dynamics of vibrational relaxation T_1 and T_2 proceeds on a much slower time scale and the relation $T_1 > T_2$, valid in liquids, may not be fulfilled. Additionally, it can be expected that the rigid environment of the solute leads to significant inhomogeneous band broadening in glasses. Although a general outline of the dynamics in glasses has been developed,[26,27] the fundamental issues of vibrational dynamics remain to be clarified. There is a limited number of papers on vibrational relaxation in glasses.[5]

To explain the spectacular changes in the bandwidths and band shapes of the ν_S(C≡C) stretching mode of phenylacetylene in benzene, we have to understand the mechanisms of vibrational relaxation which are responsible for the band broadening in the frequency domain.

First, we will discuss the mechanisms of band broadening in liquid phase at room temperature. We have applied the hard collision model,[11,12] which belongs to the group of homogeneous vibrational dephasing mechanisms, and the theoretical results have been compared with the experimental data for phenylacetylene solutions in benzene.

In Figure 7 we show the experimental bandwidths of the isotropic component of the ν_S(C≡C) stretching mode of phenylacetylene in benzene compared with the theoretical bandwidth for $T = 298$ K calculated from the hard collision model[11,12] in the same way as in our previous paper for the PA−methylcyclohexane system.[4] All the parameters for PA were unchanged and are the same as in ref 4, the hard sphere

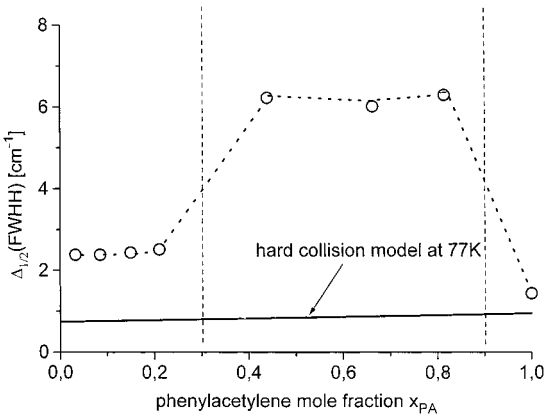

Figure 8. Raman isotropic bandwidth $\Delta_{1/2}$(fwhh) of the C≡C stretching mode of phenylacetylene in benzene as a function of phenylacetylene mole fraction x_{PA}: ○, experimental data at 77 K; —, hard collision theoretical model.[11,12]

diameter of benzene was estimated to be 5.13 Å, $L_{ik} = (5.9 + 5.13)/2 \times 18.0 = 0.306$ Å. The concentration dependence of the theoretical bandwidth was fitted with the linear equation $\Delta_{1/2}^{theo}(\text{fwhh})(\text{cm}^{-1}) = 8.24 + 1.89x_{PA}$, while the experimental one was fitted with $\Delta_{1/2}^{exp}(\text{fwhh})(\text{cm}^{-1}) = 5.69 + 1.54x_{PA}$. The hard repulsive collision model predicts the bandwidths to be about 2.5 cm^{-1} larger than those observed experimentally, but the concentration dependence is reproduced fairly well. Although the hard repulsive collision model overestimates the experimental magnitudes, which may be due to the uncertainties in estimation of the theoretical parameters used in the model, it seems that the model predicts rather reasonably the experimental bandwidths for PA in benzene in the liquid phase. This conclusion is similar to that obtained in ref 4 for PA in methylcyclohexane in liquid solution. However, there is some inconsistency in this conclusion in comparison with the observed experimental Gaussian band shapes for PA in benzene (Figure 2) instead of Lorentzian ones which correspond to the homogeneous mechanism of vibrational dephasing.

To learn more about mechanisms of band broadening in frozen matrixes at low temperature we have applied the hard repulsive collision model for PA in benzene at 77 K. The results are presented in Figure 8, where we have compared the experimental data for PA in benzene at 77 K and the theoretical bandwidths calculated from the hard, repulsive collision model[11,12] at 77 K. It is evident from Figure 8 that the homogeneous broadening due to the hard collision model cannot be applied and a quite different mechanism of broadening must operate. However, it should be noticed that for concentrations lower than about $x_{PA} = 0.3$ the hard collision model predicts the concentration dependence and the absolute magnitude of the bandwidth for neat PA ($x_{PA} = 1.0$). The theoretical values for the concentrations between $x_{PA} = 0.0$ and 0.3 are lower than the experimental ones, giving only about half of the experimental bandwidth, but taking into account the approximations which were used to calculate the bandwidths at low temperature, they seem to be quite reasonable. Taking into account that the hard collision model predicts a temperature dependence of $\Delta_{1/2}^{theo}(\text{fwhh})(\text{cm}^{-1}) \propto \rho^{T3/2}g(\sigma)$, where ρ and $g(\sigma)$ are the density of the solution and the radial distribution function, we have assumed that $g(\sigma)$ and the hard sphere diameter σ are temperature independent, which may be a crude approximation. The experimental bandwidths in concentration range between about $x_{PA} = 0.3$ and 0.9 demonstrate a rapid increase, and their magnitudes are comparable to those observed in liquid phase of PA in benzene solutions at the same concentrations. This implies that an additional mechanism of vibrational relaxation turns on which is linked to the onset of structural processes occurring in frozen matrixes. The results show evidently that for different concentrations in benzene different structural environments are generated around the molecular oscillator ν_S(C≡C) of phenylacetylene.

The question arises, what is the origin of the significant broadening in the region between $x_{PA} = 0.3$ and 0.9? To answer this question we should know more about the thermodynamic states of PA in frozen benzene matrixes. It would be very helpful to have access to the crystallographic and thermodynamic data as a function of concentration for PA in benzene, which are not available in the literature at present. However, combining the three important findings of this paper—(a) splitting, (b) the dramatic increase of depolarization ratios at 77 K in comparison with the liquid phase, and (c) spectacular changes in the band shapes with concentration (Figure 5)—we may suggest the possible answers. Additionally, the results we have obtained for PA in acetonitrile and methylcyclohexane in our prevous paper[5] may give some indications. We have found[5] that for PA in acetonitrile we observe the splitting into three narrow peaks (like for PA in benzene for concentrations larger than about $c = 7.699$ mol/dm^3) and a single, narrow peak for PA in methylcyclohexane (like for PA in benzene for concentrations lower than $c = 2.26$ mol/dm^3) in the whole concentration range. Methylcyclohexane is known to form glassy matrixes at 77 K, while acetonitrile is known to form a polycrystalline matrix at 77 K.

There are two possible explanations. The first one is that the crystalline phase is generated for PA in benzene at 77 K in the whole concentration range and the observed evolution of the band shape is due to the Davydov splitting effect. Davydov splitting describes the effect that occurs in crystals for each vibration, which is split into *MZ*-fold states, where *M* is the number of unit cells and *Z* is the number of molecules in the unit cell. The interaction between *Z* molecules within the unit cell creates *Z* components. The broadening of each component comes from the interactions between *M* translationally equivalent molecules forming the vibron band, with components separated typically by 10^{-2}—10^{-3} cm^{-1}. It seems that the three components observed in frozen matrixes of PA in benzene result from the interactions between *Z* molecules within the unit cell. It would mean that $Z = 3$ (or 4 as we obtained from fitting in Figure 6). Despite the splitting typical for crystalline solids, our results on mechanisms of band broadening for each component as a function of concentration discussed above seem to suggest mechanisms typical for liquids rather than crystals, with negligible contribution from vibron broadening due to the periodicity of the intermolecular potential (broadening due to *M* translational components). In the framework of this assumption about the Davydov effect, the evolution of the band shape can be explained as due to the change of the number of molecules in the unit cell *Z*. For lower concentrations of PA, $Z = 1$ and the band appears as a single peak (the first two upper profiles in Figure 5). When PA concentration increases, *Z* may also increase, leading to the appearance of additional components due to $Z = 2$ or 3 interactions in the cells. This effect can be seen for the profiles at $c = 1.63$ and 2.26 mol/dm^3 in Figure 5, demonstrated by a significant intensity increase on the red side of the band. For PA concentrations going from $c = 4.501$ to 7.699 mol/dm^3 the intensity on the red side increases dramatically (because most of the molecular oscillators feel the interactions with $Z = 3$ or 4 molecules in the cell) leading to the red-shifting of the maximum peak position. The bands

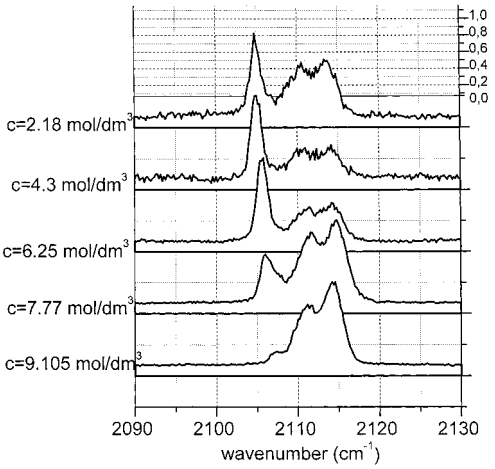

Figure 9. VV Raman spectra of the C≡C stretching mode of phenylacetylene in benzene at 77 K at a few concentrations (slow freezing) (c = 2.18, 4.30, 6.25, 7.77, 9.105 mol/dm^3 going from top to bottom).

become broad due to the splitting into three (or four) components, although the structure due to splitting cannot be seen yet because the subbands are still relatively broad. When PA concentration goes up further, the three components become narrower, revealing the splitting into three bands separated by about 5 cm^{-1}. The narrowing of the subbands may come from increasing order with increasing PA concentration. The increasing order would reduce the inhomogeneous contribution, which corresponds well with the results in Figure 8. We have shown that the hard collision model reproduces only about half of the total bandwidth for PA concentrations between $x_{PA} = 0.0$ and 0.3. The second half may come from inhomogeneous broadening. For PA concentrations larger than $x_{PA} = 0.9$, the hard collision model reproduces the whole bandwidth. The increasing order in PA solutions on going from the liquid phase to the solid phase at 77 K is suggested by the dramatic increase of the depolarization ratios $\rho = I_{VH}/I_{VV}$ from 0.147 to 0.735.

To determine if the Davydov effect leads to the band splitting, we are only studying the band shape in isotopic mixtures as a function of composition. The results will be published in a subsequent paper. The effectiveness of isotopic mixture crystal studies for determining the nature of the splitting is very important because the multiplet structure of the neat crystal is perturbed severely in the isotopic mixed crystals for Davydov splitting.

The second possible explanation of the experimental results of this paper is the existence of three different phases in frozen matrixes, glassy, isotropic (similar to that in liquid phase), and crystalline ones. This suggestion seems to be supported by our observation that the phases which are generated in PA frozen benzene matrices strongly depend on the method of freezing. It seems that the phase generated through rapid freezing obtained by immersion of the sample in liquid nitrogen is different from that obtained by slow freezing through a gradual change of temperature. The results we have presented so far were obtained by rapid freezing. In Figure 9 we have shown the VV Raman profiles for PA in benzene at 77 K when the sample was frozen slowly. Like in Figure 5 we observed a single peak for lower PA concentrations with an increasing band structure on the blue frequency side. However, the single peak is on the red side (at about 2105 cm^{-1}) in contrast to the single peak in Figure 5 observed on the blue side (at about 2116 cm^{-1}) when the sample was frozen rapidly. Taking into accout that the single peak at about 2116 cm^{-1} is also observed for PA in glassy methylcyclohexane, while the peak at about 2105 cm^{-1} is observed in polycrystalline acetonitrile,[5] it may be suggested that the peak at 2105 cm^{-1} corresponds to the crystalline phase, the peak at 2116 cm^{-1} to the glassy phase, and the peak in the middle at about 2110 cm^{-1} to the isotropic phase similar to that observed in the liquid phase. The different behavior with the cooling rate can be understood in terms of the structure of glassy and crystalline materials. When rapid cooling occurs to a temperature at which the crystalline state is expected to be more stable, molecular movement is too slow or the geometry too awkward to take up a crystalline conformation. In another words, a path to the state of lowest energy might not be available at rapid cooling and a glassy state is produced instead of a crystalline one. Thus, the term glassy is synonymous with a persistent nonequilibrium state with random arrangement. On the other side, the term isotropic phase at 77 K used here represents the equilibrium state at 77 K with the random arrangement characteristic of the liquids. This phase is produced for that fraction of molecules from the whole Boltzmann distribution at 293 K that have the energies of molecular movements large enough in order to follow the relaxation channels and paths of energy dissipation to preserve the equilibrium distribution of states at 77 K.

Assuming the coexistence between these three phases for PA in benzene, we can rationalize the experimental findings in Figures 5 and 9 in the following way. The evolution of the band shape in Figure 5 reflects the increasing contribution from the crystalline phase going to the glassy phase for lower PA concentrations to nearly equal contribution from three different environments, glassy, isotropic, and crystalline ones. On the other hand, slow freezing generates low PA concentrations in benzene mainly from the crystalline phase with its contribution decreasing with increasing PA concentration accompanied by the increasing contribution from the isotropic and glassy phase.

However, the third explanation should be also taken into account. It is interesting to notice that the band of the PA stretching mode ν_S(C≡C) in liquid solutions shows significant asymmetry on the red frequency side. It may be due to hot bands, but the asymmetric band shape may also reflect the existence of two or three peaks of similar origin to those we observed at 77 K. The structure in liquid solutions cannot be seen because of significant components band broadening at room temperature. When the temperature goes down, the components become narrower, revealing the splitting. It may suggest that the structural order of PA in liquid benzene solutions and in frozen matrixes at 77 K are in fact very similar. To exclude this hypothesis, the time-resolved hole-burning experiments would be very helpful, similar to those performed for studying the structure of water.[28]

5. Conclusions

In this paper the results on vibrational dynamics of phenylacetylene in frozen benzene matrixes at 77 K are presented and compared with the results in liquid solutions at room temperature. The main focus of the proposed experimental studies was to learn more about intermolecular structure and dynamics of PA in different condensed phase environments. Solute concentrations were varied in order to assess the role of solute−solute interactions and to determine if and under what conditions ordering occurs. The temperature effect on vibrational spectra was determined and analyzed.

We have found that the isotropic Raman band broadening of the PA stretching mode ν_S(C≡C) in liquid benzene solutions at room temperature is dominated by pure vibrational dephasing

due to hard-sphere repulsive interactions. In contrast, for PA in frozen matrixes at 77 K, the vibrational relaxation mechanism strongly depends on benzene concentrations. For PA concentrations lower than about $x_{PA} = 0.3$, the mechanism of pure vibrational dephasing due to hard-sphere repulsive interactions seems to reproduce only about half of the total bandwidth. The second half may be due to inhomogeneous band broadening.

For PA concentrations larger than $x_{PA} = 0.9$ the hard collision model reproduces the whole bandwidth, suggesting that the inhomogeneous contribution disappears due to increasing order in the system. For the PA concentration region between $x_{PA} = 0.3$ and $x_{PA} = 0.9$, the bands demonstrate a rapid, significant broadening, which implies that an additional mechanism of vibrational relaxation turns on which is linked to the onset of structural processes occurring in frozen matrixes. The results show evidently that for different PA concentrations in benzene different structural environments are generated around the molecular oscillator ν_S(C≡C) of phenylacetylene.

The results presented here include three important findings: (1) the depolarization ratios ($\rho = I_{VH}/I_{VV}$) are temperature-dependent, and the isotropic Raman component practically disappears at 77 K, (2) spectacular changes in the Raman band shapes are observed with concentration at 77 K, and (3) splitting of the band of the PA ν_S(C≡C) mode into three bands is observed.

Our results show a marked increase in the depolarization ratios in going from liquid solution to frozen benzene matrixes. This increase in ρ may be taken as evidence of increased ordering of PA in frozen matrixes. At 77 K, the depolarization ratios of PA in benzene are about 0.735, being as much as 5 times as large as in liquid benzene. This may suggest a high degree of alignment at 77 K. At this stage it is unclear what the structure of PA in frozen benzene is and to what extent the observed spectra are a manifestation of solute−solute interactions typical for nematic materials and the resulting structuring. However, our results show evidently that PA in benzene solutions and pure PA have properties between those of isotropic liquids, glassy, and crystalline solids. We have shown that the mechanisms of vibrational dephasing in liquid and solid PA solutions for some concentrations are similar and typical for isotropic liquids. On the other side, we have found the splitting of the PA ν_S(C≡C) band and the change of the depolarization ratio with temperature and concentration, indicating anisotropic properties typical for crystals. We have found and estimated the contribution coming from inhomogeneous band broadening in some PA concentration ranges.

The results presented here and current interpretations clearly illustrate that additional elaborated methods to estimate the degree of ordering and supplementary evidence from crystallographic data for these systems are required. Further studies are needed to determine which types of solute−solute and solute−solvent intermolecular forces are chiefly responsible. Computer modeling and simulation as well as crystallographic studies would be very helpful in answering these questions.

Acknowledgment. The authors gratefully acknowledge the support of this work by KBN through grants 020/*T*09/97/12, Polish-American grant of M. Sklodowska-Curie Fund II, and Deutscher Academischer Austauschdienst (DAAD) fellowship. Support from the Dz.S. 559/99 is also acknowledged.

References and Notes

(1) Drzaic, P. S. *Liquid crystal dispersions*; Series on Liquid Crystals; 1995; Vol. 1.

(2) *Infrared and Raman Spectroscopy*; Schrader, B., Ed.; VCH: New York, 1995. Pershan, P. S. Raman studies of orientational order in liquid crystals. In *The molecular physics of liquid crystals*; Luchhurst, G. R., Gray, G. W., Eds.; Academic: London, p 385.

(3) Abramczyk, H.; Kolodziejski, M.; Waliszewska, G. *Chem. Phys*. **1998**, *228*, 313.

(4) Kolodziejski, M.; Waliszewska, G.; Abramczyk, H. *J. Phys. Chem.* **1998**, *102*, 1918.

(5) Abramczyk, H.; Kolodziejski, M.; Waliszewska, G. *J. Phys. Chem.* **1998**, *102*, 7765.

(6) Cates, D. A.; Mac Phail, R. A. *J. Phys. Chem.* **1991**, *95*, 2209.

(7) Ben-Amotz, D.; Lee, M. R.; Cho, S.; List, D. *J. Chem. Phys*. **1992**, *96*, 8781.

(8) *Topics in Applied Physics, Vol. 60, Ultrashort Laser Pulses and Applications*; Kaiser, W., Ed.; Springer-Verlag: New York, 1988.

(9) Lynden-Bell, R. M. *Mol. Phys.* **1977**, *33*, 907.

(10) Oxtoby, D. W. *J. Chem. Phys*. **1979**, *70*, 2605.

(11) Fischer, S. F.; Laubereau, A. *Chem. Phys. Lett*. **1975**, *35*, 6.

(12) Schweizer, K. S.; Chandler, D. *J. Chem. Phys*. **1982**, *76*, 2296.

(13) Dijkman, F. G.; van Maas, J. H. *Appl. Spectrosc*. **1976**, *30*, 545.

(14) Kolodziejski, M.; Waliszewska, G.; Abramczyk, H. *Chem. Phys*. **1996**, *213*, 341.

(15) Ladanyi, B. M.; Geiger, L. C.; Zerda, T. W.; Song, X.; Jonas, J. *J. Chem. Phys*. **1988**, *89*, 660.

(16) Geiger, L. C.; Ladanyi, B. M. *J. Chem. Phys*. **1988**, *89*, 6588.

(17) Ladanyi, B. M.; Stratt, R. M. *J. Phys. Chem. A* **1998**, *102*, 1068.

(18) Rotschild, W. G. *Dynamics of Molecular Liquids*; Wiley: New York, 1984.

(19) Muller, L. J.; Vanden Bout, D.; Berg, M. *J. Chem. Phys*. **1993**, *99*, 810.

(20) Tokmakoff, A.; Fayer, M. D. *Acc. Chem. Res*. **1995**, *28*, 437.

(21) Bellows, J. C.; Prasad, P. N. *J. Chem. Phys*. **1979**, *70*, 1864.

(22) Hesp, B. H.; Wiesma, D. A. *Chem. Phys. Lett*. **1980**, *75*, 423.

(23) Prasad, P. N.; Kopelman, R. *J. Chem. Phys*. **1973**, *58*, 126.

(24) Chronister, E. L.; Dlott, Dana D. *J. Chem. Phys*. **1983**, *79*, 5286.

(25) Hill, J. R.; Chronister, E. L.; Chang, Ta-Chau; Kim, H.; Postlewaite, J. C.; Dlott, D. D. *J. Chem. Phys*. **1988**, *88*, 949.

(26) Angell, C. A.; Poole, P. H.; Shao, J. *Nuovo Cimento* **1994**, *16D*, 993.

(27) Angell, C. A. *J. Phys. Chem*. **1982**, *86*, 3845.

(28) Bratos, S.; Laubereau, A. *Theoretical Treatments of Hydrogen Bonding*; Dušan Hadži, Ed.; John Wiley & Sons: New York, 1997; p 1190.